10-2017

# HMGB1-RAGE Pathway Drives Peroxynitrite Signaling-Induced Ibd-Like Inflammation in Murine Nonalcoholic Fatty Liver Disease

Varun Chandrashekaran

Ratanesh K. Seth
*University of South Carolina*, sethr@mailbox.sc.edu

Diptadip Dattaroy

Firas Alhasson

Jacek Ziolenka
*Medical College of Wisconsin*

*See next page for additional authors*



## Publication Info

Published in *Redox Biology*, Volume 13, 2017, pages 8-19.

Redox Biology 13 (2017) 8–19

Contents lists available at ScienceDirect

Redox Biology

journal homepage: www.elsevier.com/locate/redox

Research Paper

# HMGB1-RAGE pathway drives peroxynitrite signaling-induced IBD-like inflammation in murine nonalcoholic fatty liver disease

Varun Chandrashekaran[a], Ratanesh K. Seth[a], Diptadip Dattaroy[a], Firas Alhasson[a], Jacek Ziolenka[b], James Carson[c], Franklin G. Berger[d], Balaraman Kalyanaraman[b], Anna Mae Diehl[e], Saurabh Chatterjee[a,*]

[a] Environmental Health and Disease Laboratory, Departments of Environmental Health Sciences, University of South Carolina, Columbia, SC 29208, USA
[b] Free Radical Research Center, Department of Biophysics, Medical College of Wisconsin, Milwaukee, WI, USA
[c] Exercise Science, Arnold School of Public Health, University of South Carolina, Columbia, SC 29208, USA
[d] Department of Biological Sciences and Center for Colon Cancer Research, University of South Carolina, SC 29208, USA
[e] Division of Gastroenterology, Duke University, Durham, NC 27707, USA

ARTICLE INFO

*Keywords:*
Nonalcoholic steatohepatitis
DAMP
FBA
TLR4
Flotillin
NADPH oxidase

ABSTRACT

Recent clinical studies found a strong association of colonic inflammation and Inflammatory bowel disease (IBD)-like phenotype with NonAlcoholic Fatty liver Disease (NAFLD) yet the mechanisms remain unknown. The present study identifies high mobility group box 1 (HMGB1) as a key mediator of intestinal inflammation in NAFLD and outlines a detailed redox signaling mechanism for such a pathway. NAFLD mice showed liver damage and release of elevated HMGB1 in systemic circulation and increased intestinal tyrosine nitration that was dependent on NADPH oxidase. Intestines from NAFLD mice showed higher Toll like receptor 4 (TLR4) activation and proinflammatory cytokine release, an outcome strongly dependent on the existence of NAFLD pathology and NADPH oxidase. Mechanistically intestinal epithelial cells showed the HMGB1 activation of TLR-4 was both NADPH oxidase and peroxynitrite dependent with the latter being formed by the activation of NADPH oxidase. Proinflammatory cytokine production was significantly blocked by the specific peroxynitrite scavenger phenyl boronic acid (FBA), AKT inhibition and NADPH oxidase inhibitor Apocynin suggesting NADPH oxidase-dependent peroxynitrite is a key mediator in TLR-4 activation and cytokine release via an AKT dependent pathway. Studies to ascertain the mechanism of HMGB1-mediated NADPH oxidase activation showed a distinct role of Receptor for advanced glycation end products (RAGE) as the use of inhibitors targeted against RAGE or use of deformed HMGB1 protein prevented NADPH oxidase activation, peroxynitrite formation, TLR4 activation and finally cytokine release. Thus, in conclusion the present study identifies a novel role of HMGB1 mediated inflammatory pathway that is RAGE and redox signaling dependent and helps promote ectopic intestinal inflammation in NAFLD.

## 1. Introduction

Recent clinical reports suggest intestinal inflammation, Inflammatory bowel disease-like phenotype (IBD) and neoplasia in NAFLD cases [1–3]. These reports are in addition to the comorbidities in cardiovascular system associated with fatty liver disease [4]. Emerging data have highlighted the co-existence of non-alcoholic fatty liver disease (NAFLD) and inflammatory bowel disease; both of which are increasingly prevalent disorders with significant complications and impact on future health burden [3]. With colorectal cancer the second leading cause of morbidity and mortality, the clinical finding of colonic inflammation and neoplasia in NAFLD is very significant [2,5]. The report also finds the association between nonalcoholic steatohepatitis, the active form of NAFLD and colorectal neoplasms to be independent of demographics and metabolic factors [2]. Although reports of a strong intestinal inflammatory phenotype in NAFLD/NASH cases and a mutual co-existence of liver inflammation in inflammatory bowel disease exist, the cause of such ectopic manifestation remain poorly understood [3].

NAFLD has been shown to increase circulatory levels of cytokines including adipokine leptin in the circulation, with the latter being proinflammatory in nature [6]. However, evidence of leptin resistance due to the attenuation of the JAK/STAT signaling pathway in peripheral tissues dampen its profound role in the intestine [7,8]. Recent reports of other soluble molecular mediators of inflammation in NAFLD

* Corresponding author.
*E-mail address:* schatt@mailbox.sc.edu (S. Chatterjee).

http://dx.doi.org/10.1016/j.redox.2017.05.005
Received 12 April 2017; Received in revised form 1 May 2017; Accepted 5 May 2017
Available online 10 May 2017

have emerged. These include several damage associated molecular patterns like HMGB1, uric acid, extracellular ATP and NAD and has been found to be prime causes of sterile inflammation in the liver and other peripheral organs [9–17].

NAFLD/ NASH have often been associated with hepatocyte necrosis primarily from abnormal triglyceride metabolism and resultant lipotoxicity [18]. Further, there is a tight link between JNK1-dependent HMGB1 secretion from lipotoxic hepatocytes and a paracrine cytolytic effect on neighboring cholesterol-loaded hepatocytes operating via TLR4 [18]. Interestingly HMGB1 can bind to TLR4 and generate a similar inflammatory response though the binding of lipopolysaccharide is preferred over HMGB1 [19].

High mobility group box 1 (HMGB1) is a non-histone protein involved in maintaining the architecture of chromatin. HMGB1 also acts extracellularly as a cytokine, in processes such as inflammation, cell migration and stem cell recruitment. Plasma HMGB1 level at admission is an indicator of the severity of illness and a useful mortality predictor in exertional heatstroke [20]. HMGB1 circulatory levels have been predictors of outcome in neuroinflammation, ischemia reperfusion injury and sepsis [11,21–25]. We and others have shown that HMGB1 circulatory levels are increased in NASH and are found to contribute in the pathology of liver lobule and tubular toxicity [11,15].

Though circulatory levels of HMGB1 has been associated with pathology, the signaling pathways, its association with pattern recognition receptors in the intestine following liver injury has never been explored. HMGB1 can bind to both TLR4 and RAGE and has been extensively reviewed by Weber et. al [19]. Their binding abilities depend on the redox states of HMGB1 [19]. The reduced form contains a thiol group at all three cysteine residues with a serum half-life of 17 min. It is this form that can bind to RAGE and activate inflammatory pathways [19]. The present study tested the hypothesis that NAFLD leads to an increase in circulatory HMGB1 levels triggering inflammatory pathways in the intestine. Mechanistically HMGB1 binds to RAGE in the distal intestine and activates TLR4 translocation to lipid rafts via a peroxynitrite dependent manner. The study reports a novel redox-immune crosstalk in a murine model of NAFLD and helps understand a possible complicated relationship of innate immune interaction in NAFLD-induced ectopic intestinal inflammation and IBD-like phenotype.

## 2. Materials and methods

### 2.1. Animal model

#### 2.1.1. Mice model for NAFLD

Pathogen-free, adult, male mice with C57BL/6J background (Jackson Laboratories, Bar Harbor, ME) were used in the study. They were fed with a high-fat diet (60% kcal fat) (Research diets, New Brunswich, NJ) for 18 weeks and used as a model of nonalcoholic fatty liver disease (NAFLD). Mice kept on a similar diet for 4 weeks served as a model for early NAFLD (DIO) where mild steatosis was evident with no liver inflammation, normal chow diet was used as a model of lean controls. Mice that contained the disrupted p47 phox (B6.129S2-Ncf1$^{tm1shl}$ N14) gene were treated like the NAFLD group (Supplementary material). All groups of mice had ad libitum access to food and water. All animals were treated in strict accordance with the NIH Guide for the Humane Care and Use of Laboratory Animals, and the experiments were approved by the institutional review board at the University of South Carolina at Columbia.

#### 2.1.2. Immunohistochemistry and immunofluorescence

Formalin-fixed, paraffin-embedded intestinal and liver tissue from all the mice groups were cut into 5 μm thick tissue sections. Each section was deparaffinized (Supplementary material). Epitope retrieval of deparaffinized sections was carried out using epitope retrieval solution and steamer (IHC-World, Woodstock, – MD) following the manufacturer's protocol. The primary antibodies were used at 1:250 dilutions. Antigen-specific immunohistochemistry was performed using Vectastain Elite ABC kit (Vector Laboratories, Burlingame, CA) following manufacturer's protocols. 3,3′ Diaminobenzidine (Sigma-Aldrich) was used as a chromogen substrate. Sections were counter-stained by Mayer's hematoxylin (Sigma-Aldrich). For immunofluorescence assays the cells were then incubated with compatible AlexaFlour conjugated secondary antibodies from Invitrogen. (Grand Island, NY), followed by three washes in PBSTx for 10 min each. Finally, the cells were mounted in Prolong gold antifade reagent with DAPI. Images were taken under 40X and 60X objective using the Olympus BX51 microscope.

#### 2.1.3. Quantitative RT-PCR

Gene expression levels in tissue samples were measured by two-step qRT-PCR. Total RNA was isolated from liver, small intestine tissue and cells grown in a monolayer by homogenization in TRIzol reagent (Invitrogen) per the manufacturer's instructions and purified with the use of RNeasy mini kit columns (Qiagen, Valencia, CA). Purified RNA (1 μg) was converted to cDNA using iScript cDNA synthesis kit (Bio-Rad) following the manufacturer's standard protocol. qRT-PCR was performed with the gene-specific primers using SsoAdvanced SYBR Green supermix (Bio-Rad) and CFX96 thermal cycler (Bio-Rad). Threshold Cycle (Ct) values for the selected genes were normalized against 18S (internal control) values in the same sample. The relative fold change was calculated by the $2^{-\Delta\Delta Ct}$ method (Table 1).

#### 2.1.4. Western Blotting

SDS PAGE-Resolved protein bands were transferred to nitrocellulose membrane using precut nitrocellulose/filter paper sandwiches (Bio-Rad Laboratories, Hercules, CA) and Trans-Blot Turbo transfer system (Bio-Rad) in case of low molecular weight proteins and using wet transfer module from Invitrogen for high molecular weight proteins. Primary antibodies (Abcam) were used at recommended dilutions, and compatible horseradish peroxidase-conjugated secondary antibodies were used. Pierce ECL Western Blotting substrate (Thermo Fisher Scientific, Rockford, IL) was used for detection. The blot was imaged using G:Box Chemi XX6 (Syngene imaging systems) and subjected to densitometry analysis using Image J.

**Table 1**
Primer sequences for the genes used for real time mRNA quantitation.

| Target | Species | Sequence 5′-3′ |
|---|---|---|
| HMGB1 F | *Mus musculus* | GGACTCTCCTTTAACCGC |
| HMGB1 R | *Mus musculus* | TTGTGATAGCCTTCGCTGGG |
| MCP-1 F | *Mus musculus* | GTAGCAGCAGGTGAGTGGGGC |
| MCP-1 R | *Mus musculus* | CACAGTTGCCGGCTGGAGCAT |
| IL-1β F | *Mus musculus* | CCTCGGCCAAGACAGGTCGC |
| IL-1β R | *Mus musculus* | TGCCCATCAGAGGCAAGGAGGA |
| TGF-β F | *Mus musculus* | CTCACCGCGACTCCTCCTGCTGC |
| TGF-β R | *Mus musculus* | TCGGAGAGCGGGAACCCTCG |
| IFN-γ F | *Mus musculus* | TGCGGGGTTGTATCTGGGGGT |
| IFN-γ R | *Mus musculus* | GCGCTGGCCCGGAGTGTAGA |
| RAGE F | *Mus musculus* | CTGGTGGGACTGTGACCTTG |
| RAGE R | *Mus musculus* | CCTCTGCCTGTCATTCCTAGC |
| 18SF | *Mus musculus* | TTCGAACGTCTGCCCTATCAA |
| 18SR | *Mus musculus* | ATGGTAGGCACGGCGATA |
| IL-1β F | *Rattus norvegicus* | CCCTGCAGCTGGAGAGTGTGG |
| IL-1β R | *Rattus norvegicus* | TGTGCTCTGCTTGAGAGGTGCT |
| IL-6 F | *Rattus norvegicus* | CGAGCCCACCAGGAACGAAAGTC |
| IL-6 R | *Rattus norvegicus* | CTGGCTGGAAGTCTCTTGCGGAG |
| P47Phox F | *Rattus norvegicus* | AGCCCTGACTCAAAGGGTGA |
| P47Phox R | *Rattus norvegicus* | TAGTCCTGATCCCACCCCTA |
| MCP-1 F | *Rattus norvegicus* | TAGCATCCACGTGCTGTCTC |
| MCP-1 R | *Rattus norvegicus* | CAGCCGACTCATCATTGGGATCA |
| 18SF | *Rattus norvegicus* | GGATCCATTGGAGGGCAAGT |
| 18SR | *Rattus norvegicus* | ACGAGCTTTTTAACTGCAGCAA |

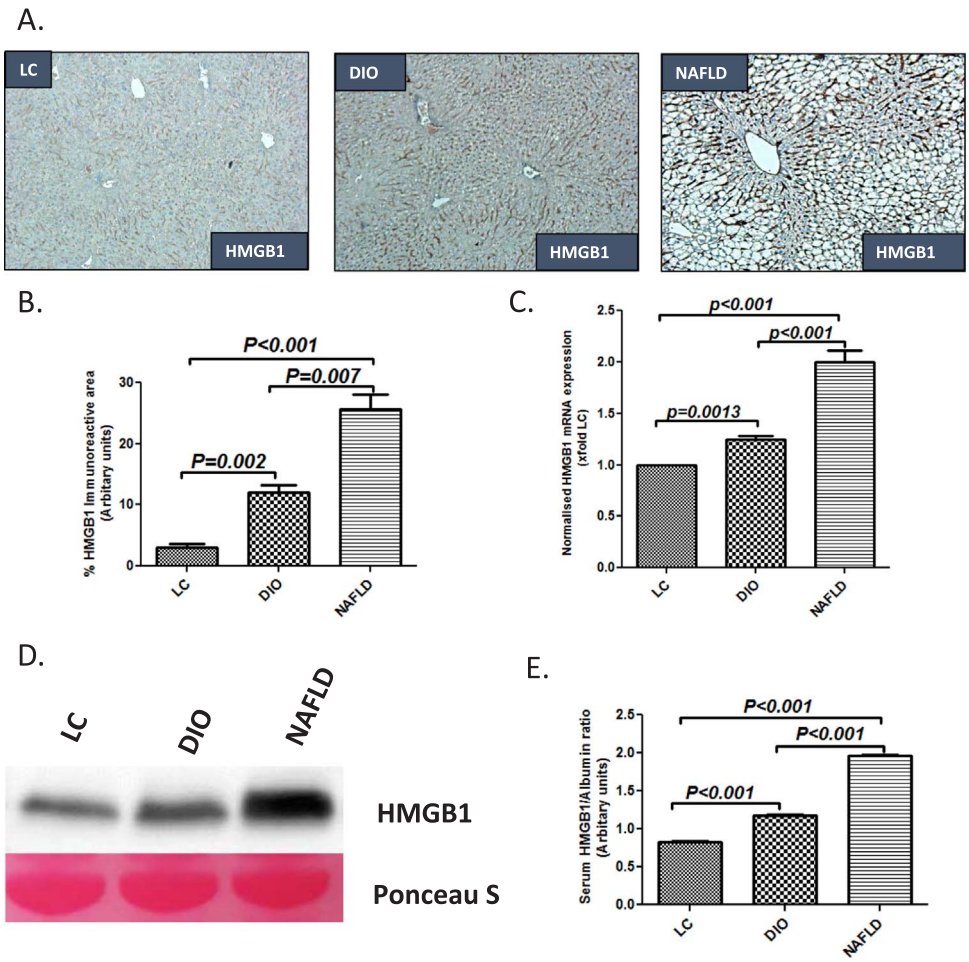


**Fig. 1.** NAFLD liver leads to HMGB1 release in the blood. A. HMGB1 immunoreactivity as shown by immunohistochemistry in liver slices from mice fed with chow diet as a model of lean control (LC), high-fat diet (60% kcal fat) for 4 weeks as a model of early NAFLD (DIO) and 16 weeks as a model nonalcoholic fatty liver disease (NAFLD). Images were taken at 20× magnification. B. Morphometric analysis of HMGB1 immunoreactivity (mean data from three separate microscopic fields were plotted on Y-axis in LC, DIO and NAFLD groups of mice (**P < 0.05, ***P < 0.01)). C. mRNA expressions of HMGB1 in liver tissue of LC, DIO and NAFLD groups of mice assessed by quantitative real time PCR, the expressions were normalized with 18 s and compared to the LC group and represented as fold changes to LC (**P < 0.05, ***P < 0.01). D. Western blot analysis of HMGB1 protein levels in the serum. Lanes 1–3 represent LC, DIO and NAFLD groups E. Band quantification of the HMGB1 immunoblot in LC, DIO and NAFLD groups of mice, data was normalized against Albumin (**P < 0.05, ***P < 0.01).

*2.1.5. Cell culture*

Immortalized rat intestinal epithelial cells (IEC-6) were purchased from ATCC (CRL-1592) was maintained in high glucose Dulbelcos modified eagles medium (DMEM), Corning (Tewksbury, MA) supplemented with 10% fetal bovine serum (FBS), Atlanta biologicals (Norcross, GA) suplimented with 2 mM glutamine, 0.1 U/ml Insulin, 100 U/ml Penicillin, and 100 µg/ml streptomycin; Gibco (Grand Island, NY) at 37 °C in a humidified atmosphere of 5% $CO_2$. The cells were then treated with recombinant rat HMGB1 (Mybiosource. San Diego, CA) 30 ng/ml a cytokine mediator of inflammation released by activated macrophages able to bind to and activate RAGE & TLR4, Apocynin (Sigma-Aldrich) 100 µM an inhibitor of NADPH oxidase activity and thus preventing production of superoxide, RAGE antagonist (FPS-ZM1, Milipore, MA) 200 nM V-domain ligand binding RAGE inhibitor, Peroxynitrite (Cayman Chem, Ann Arbor, MI) 300 µM a highly reactive structural isomer of nitrate, Phenyl Boronic Acid (FBA) (Sigma Aldrich) 100 µM was used as a scavenger for Peroxynitrite, PI3K inhibitor (LY294002, Sigma Aldrich) 10 µM as an inhibitor for AKT phosphorylation as required.

*2.1.6. Statistical analysis*

All experiments were repeated three times with 3 mice per group (N = 3; data from each group of mice was pooled). The statistical analysis was carried out by analysis of variance (ANOVA) followed by the Bonferroni posthoc correction for intergroup comparisons. Quantitative data from western blots as depicted by the relative intensity of the bands were analyzed by performing a student's *t*-test.

## 3. Results

Fatty liver causes the release of damage associated molecular pattern HMGB1 [11,15]. To study the levels of HMGB1 in the liver following development of fatty liver, C57BL6/J mice were fed with high fat diet for 18 weeks. HFD-fed mice showed insulin and leptin resistance, macrovesicular steatosis, inflammation and little or no fibrosis, a condition that resemble most NAFLD patients. NAFLD mice had markedly increased lobular inflammation as shown by hematoxylin eosin staining and lipid droplets when compared to both an early time point with no significant steatosis (4 weeks of HFD) (DIO group) or lean controls (LC group) (Supplementary material Fig. 1A–C). NAFLD mice showed significantly increased localization and protein levels of HMGB1 in the liver with higher immunoreactivity in both hepatocytes and sinusoidal spaces when compared to DIO ($p = 0.007$) and LC groups ($p < 0.001$) (Fig. 1A and B). mRNA expression of HMGB1 was significantly higher in the NAFLD liver when compared to both DIO and LC groups showing that HMGB1 protein was endogenous to the diseased liver (Fig. 1C). Mice with fatty liver disease (NAFLD) had significantly increased serum HMGB1 levels as analyzed by western

blot analysis and band quantification when compared with both LC (> 3 fold) and DIO (> 2 fold) groups (Fig. 1D and E).

### 3.1. Increased circulatory HMGB1 in NAFLD correlates well with peroxynitrite generation, TLR4 trafficking to lipid rafts and intestinal inflammation in a NOX2 dependent manner

To study the role of circulatory HMGB1 in NAFLD in intestinal inflammation, mouse intestinal tissue was evaluated for the mechanism of ectopic inflammation. Results showed that there was a significant increase in the levels of MCP-1, TGF-β, IL1β and IFN-γ when assessed by immunohistochemistry in the NAFLD group when compared to both LC and DIO groups (Fig. 2A). Further, mRNA levels of the above cytokines increased significantly ($p < 0.001$) in NAFLD group when compared to both LC and DIO groups respectively suggesting the endogenous nature of the inflammation (Fig. 2B). Both increased levels of mRNA and protein of the cytokines were significantly decreased ($p < 0.001$) in p47 phox knockout mice when compared to NAFLD mice suggesting that the inflammation was NOX-2 dependent (Fig. 2A and B). To study whether NOX2 was activated in the small intestine, experiments were performed to assess the membrane assembly of the NOX2 subunits p47 phox and gp91 phox using immunofluorescence microscopy and co-localization studies. Results suggested that the number of colocalization events of gp91 phox and p47 phox in the intestinal membrane were significantly higher in NAFLD group when compared to both LC and DIO groups (Fig. 2C and Supplementary material Fig. 2A) while deletion of the p47 phox gene caused a significant decrease in the membrane assembly (Fig. 2C and Supplementary material Fig. 2A) suggesting a strong NOX2 activation in the NAFLD intestine. Since we have shown the role of NOX2 in peroxynitrite formation in NAFLD, studies were conducted to show the levels of 3-nitrotyrosine in the NAFLD intestine and whether the tyrosine nitration by peroxynitrite was NOX-2 dependent. Results showed that there was a significant increase in 3-nitrotyrosine levels in the NAFLD intestine group when compared to both LC and DIO groups (Fig. 2D and Supplementary material Fig. 2B). 3-nitrotyrosine levels were significantly decreased in the P47 phox knockout mice suggesting that the tyrosine nitration from primarily peroxynitrite generation was NOX-2 dependent though other non-peroxynitrite sources of 3-nitrotyrosine generation cannot be ruled out at this point (Fig. 2D and Supplementary material Fig. 2B).

We have shown previously that NOX-2 drives TLR4 trafficking into the lipid rafts [26]. To study the role of NOX2 in TLR4 trafficking to lipid rafts and confirming the role of NOX2-mediated TLR4 pathway in inflammation of the intestine, TLR4-Flotillin colocalization were assessed in the NAFLD intestines. Results showed that the number of TLR4-Flotillin colocalizations were significantly increased in the NAFLD intestines when compared to both LC and DIO tissues (Fig. 2E and Supplementary material Fig. 2C) while there was a significant decrease in the above colocalization events in the p47 phox knock mice intestines suggesting a NOX-2 derived TLR4 trafficking (Fig. 2E and Supplementary material Fig. 2C). NAFLD group also showed higher Claudin-2 protein levels, a hallmark of IBD-like phenotype when compared to lean and DIO groups (Fig. 2F). P47 phox deletion reversed the changes observed in Claudin-2 levels (Fig. 2F).

### 3.2. HMGB1 primes NOX2 activation and TLR4-derived inflammation in intestinal epithelial cells

To study the mechanism of HMGB1 induced NOX2 activation and subsequent inflammation in the intestine, experiments were performed in intestinal epithelial cells (IE6). Results showed that cells primed with HMGB1 showed a significant increase in p47 phox-gp91 colocalization events when compared to vehicle control (Fig. 3A, Supplementary material Fig. 3A). HMGB1 primed cells treated with apocynin had significantly decreased colocalization events when compared to HMGB1-only treatment (Fig. 3A, Supplementary material Fig. 3A). HMGB1-primed cells had significantly higher immunoreactivity of tyrosine nitration indicating a possible role of peroxynitrite that is NOX2 dependent when compared to vehicle control and cells treated with apocynin (Fig. 3B, Supplementary material Fig. 3B). To confirm the role of HMGB1 in NOX2 driven TLR4 trafficking, HMGB1 primed cells were assessed for TLR4-Flotillin colocalization using immunofluorescence microscopy. Results showed that HMGB1-primed cells had significant increase in TLR4-Flotillin colocalization events when compared to vehicle control and apocynin treatment (Fig. 3C, Supplementary material Fig. 3C). The results suggested that HMGB1-mediated NOX2 was involved in TLR4 trafficking into the lipid rafts, a crucial event that drives intestinal inflammation in NAFLD.

TLR4 activation leads to an increase in the release of interleukins 1β and 6, that have been found to have profound roles in intestinal inflammation and IBD-like phenotype [27]. To study whether HMGB1-activated NOX2 was involved in the release of IL1β and IL6, mRNA expressions of these cytokines were assessed from cell lysates primed with HMGB1. Results showed that HMGB1-primed cells had significantly increased IL1β and IL6 mRNA expression when compared to vehicle control ($p < 0.001$) and HMGB1-primed cells treated with Apocynin ($p < 0.001$) (Fig. 3D and E). The results suggested that HMGB1-induced NOX2 activation increases expression of TLR4-pathway cytokines IL1β and IL6.

### 3.3. Peroxynitrite drives TLR4 trafficking into lipid rafts via the AKT pathway

Results obtained both invivo and invitro (Figs. 1–3) suggested a possible role for NOX2 derived peroxynitrite in TLR4 activation and release of IL1b and IL6. To study the involvement of peroxynitrite and its activation of AKT pathway for TLR4-trafficking into the lipid rafts, experiments were designed in vitro to confirm this mechanism. Results showed that cells primed with peroxynitrite caused a significant increase in TLR4-Flotillin colocalization events when compared to vehicle control (Fig. 4A, Supplementary material Fig. 4A). Cells primed with peroxynitrite but treated with specific peroxynitrite scavenger phenyl boronic acid (FBA) showed a significant decrease in TLR4-Flotillin colocalization events when compared to peroxynitrite-only primed cells (Fig. 4A, Supplementary material Fig. 4A). To show the role of AKT in peroxynitrite-induced TLR4 trafficking into lipid rafts, cells were treated with PI3K inhibitor. Results showed that peroxynitrite primed cells and PI3K inhibitor showed a significant decrease in TLR4 trafficking into lipid rafts as indicated by decreased TLR4-Flotillin colocalization events (Fig. 4A, Supplementary material Fig. 4A).

To show that peroxynitrite caused AKT phosphorylation in IE6 cells, experiments were performed to study the phosphorylation in AKT and was compared to total AKT levels in the cell lysate. Results showed that AKT phosphorylation peaked at 40 min post priming with peroxynitrite (Fig. 4B; Supplementary material Fig. 4B). Thus, results from Fig. 4A and B suggested a strong role of peroxynitrite-induced AKT phosphorylation in TLR4 activation a key event in IE6 cells. To study whether peroxynitrite-induced AKT phosphorylation and TL4 activation was involved in the proinflammatory phenotype in intestinal epithelial cells, mRNA expression of IL1**β** and IL6 were observed. Results showed that mRNA expression of IL1**β** and IL6 were increased significantly ($p < 0.001$) in peroxynitrite primed IE6 cells when compared to vehicle controls (Fig. 4C and D). Cell treated with peroxynitrite scavenger FBA or AKT inhibitor had significantly decreased ($p < 0.001$) expressions of IL1β and IL6 when compared to peroxynitrite-only group (Fig. 4C and D).

### 3.4. HMGB1 binding to RAGE causes NOX2 activation and peroxynitrite generation

To study the levels of RAGE in NAFLD intestines, qRTPCR was

conducted from tissue lysates. Results showed that NAFLD intestines showed a 35-fold increase in RAGE mRNA expression when compared to lean controls (Fig. 5A) and a > 2-fold increase when compared to DIO group (which does not show liver disease based on NASH scores). Intestinal epithelial cells showed a significant increase in P47Phox expression (> 5 fold) when primed with HMGB1 but had significantly decreased P47Phox expression following incubation with a specific RAGE-antagonist (Fig. 5B). IE6 cells primed with HMGB1 showed significantly increased gp91phox-p47 phox colocalization suggesting a strong NOX2 activation when compared to vehicle controls (Fig. 5C and Supplementary material Fig. 5C). To ensure the specificity of HMGB1-RAGE binding we denatured the HMGB1 by boiling the protein for 60 min. Also, we used a specific antagonist of RAGE as a dual approach. Results showed that NOX2 activation was significantly inhibited using RAGE antagonist and denatured HMGB1 as shown by decreased gp91-p47 phox colocalization events (Fig. 5C and Supplementary material Fig. 5A). Tyrosine nitration which is a possible result from peroxynitrite dependent redox pathway was significantly increased in HMGB1-primed cells when compared to vehicle controls (Fig. 5D and Supplementary material Fig. 5B). Incubation with either a specific

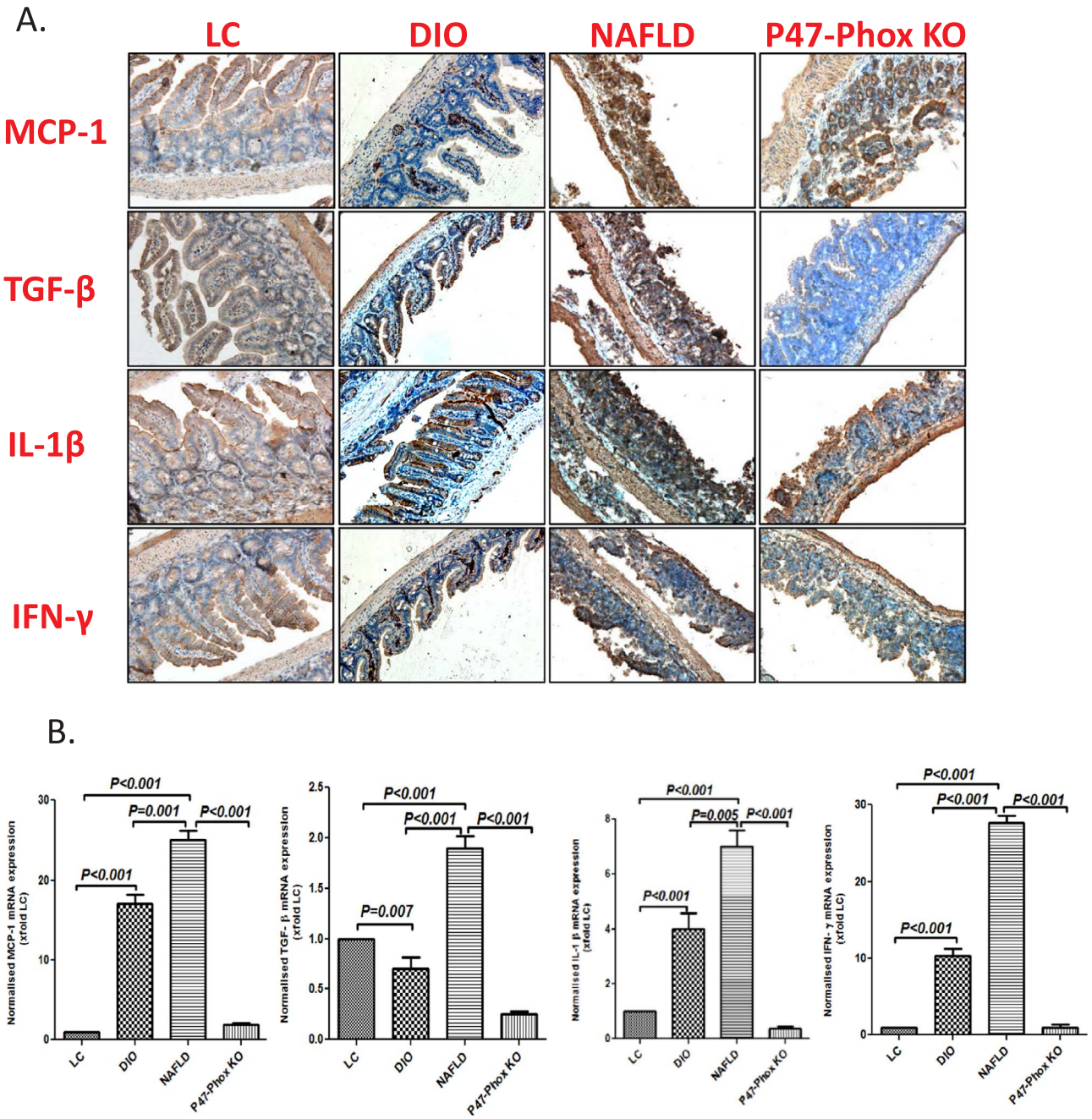


**Fig. 2.** NAFLD intestines have increased inflammation mediated by NADPH oxidase activity and TLR-4 recruitment. A.MCP-1, TGF-β, IL-1β and IFN-γ immunoreactivity as shown by immunohistochemistry in intestinal slices from LC, DIO, NAFLD mice. Mice lacking a functional P47 Phox sub-unit fed on high-fat diet (60% kcal fat) for 16 weeks (P47Phox KO). Images were taken at 20× magnification. B. mRNA expressions of MCP-1, TGF-β, IL-1β and IFN-γ in intestinal tissue of LC, DIO, NAFLD and P47Phox KO groups of mice as assessed by quantitative real time PCR, the expressions were normalized with 18 s and compared to the LC group and represented as fold changes to LC (**P < 0.05, ***P < 0.01). C. Immunofluorescence for P47Phox (Green) and GP-91 Phox (Red) co-localization in intestinal sections of LC, DIO, NAFLD and P47Phox KO mice (60× images). D. Immunofluorescence for 3-Nitro-Tyrosine (Red) in intestinal sections of LC, DIO, NAFLD and P47Phox KO mice (20×). E. Immunofluorescence for Flotilin (Green) and TLR-4 (Red) co-localization in intestinal sections of LC, DIO, NAFLD and P47Phox KO mice (60× images). F. immunofluorescence for Claudin-2 protein levels in LC, DIO, NAFLD and P47Phox KO mice (60× images) as shown by red stain. (For interpretation of the references to color in this figure legend, the reader is referred to the web version of this article.)

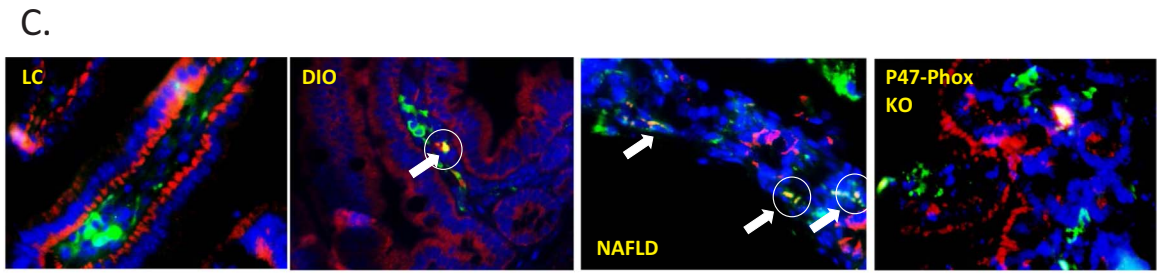


c: Co-localization of P47Phox (Green) with GP-91 Phox (Red)

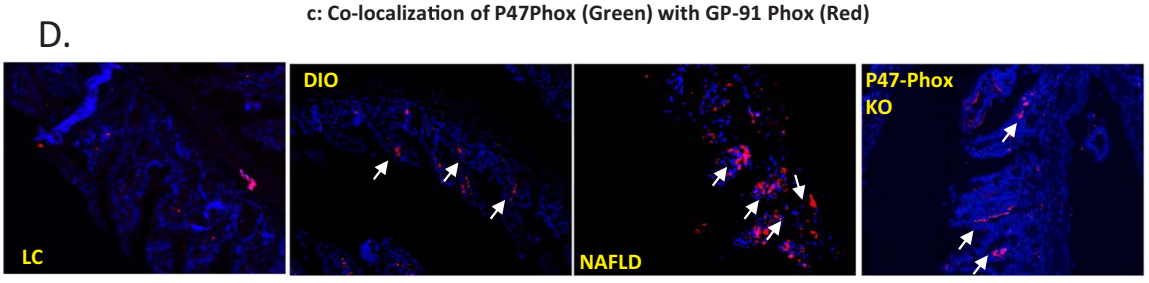


d: Immunofluorescence for 3-NitroTyrosine (Red) in small intetines

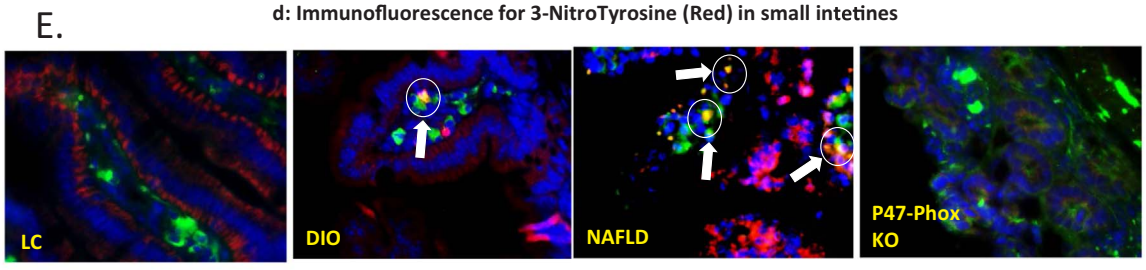


e: Co-localization of Flotilin (Green) with TLR-4 (Red)

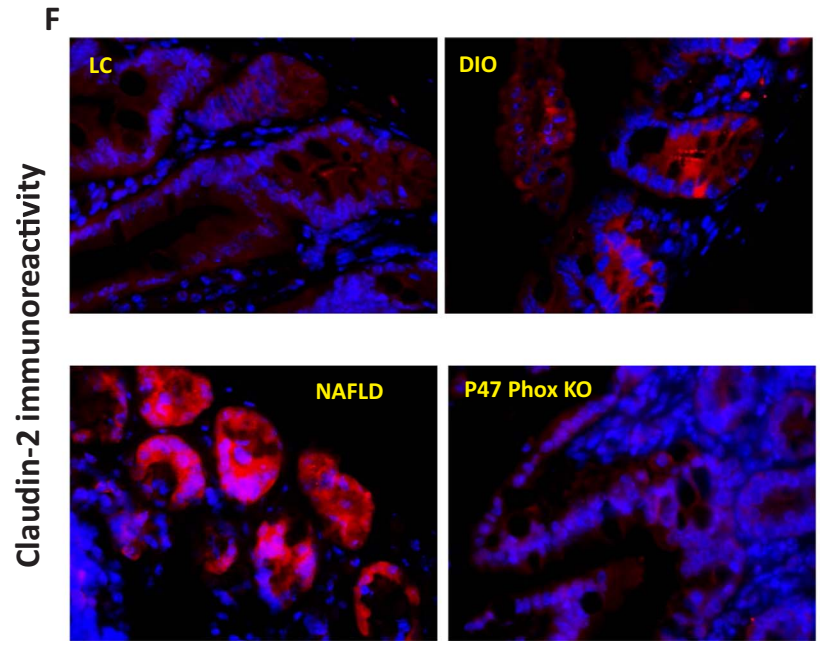


f: Immunofluorescence for Claudin-2 (Red) in small intestines

**Fig. 2.** (*continued*)

RAGE antagonist or use of denatured HMGB1 significantly decreased tyrosine nitration when compared to HMGB1 primed cells (Fig. 5D and Supplementary material Fig. 5B) suggesting that HMGB1-RAGE binding was responsible for NOX2 activation and peroxynitrite generation.

### *3.5. HMGB1 binding to RAGE causes TLR4 activation and proinflammatory cytokine release*

Following the results of HMGB1-RAGE activation of NOX2 and peroxynitrite generation, it was imperative that we study the above pathway for TLR4 activation and proinflammatory events in the

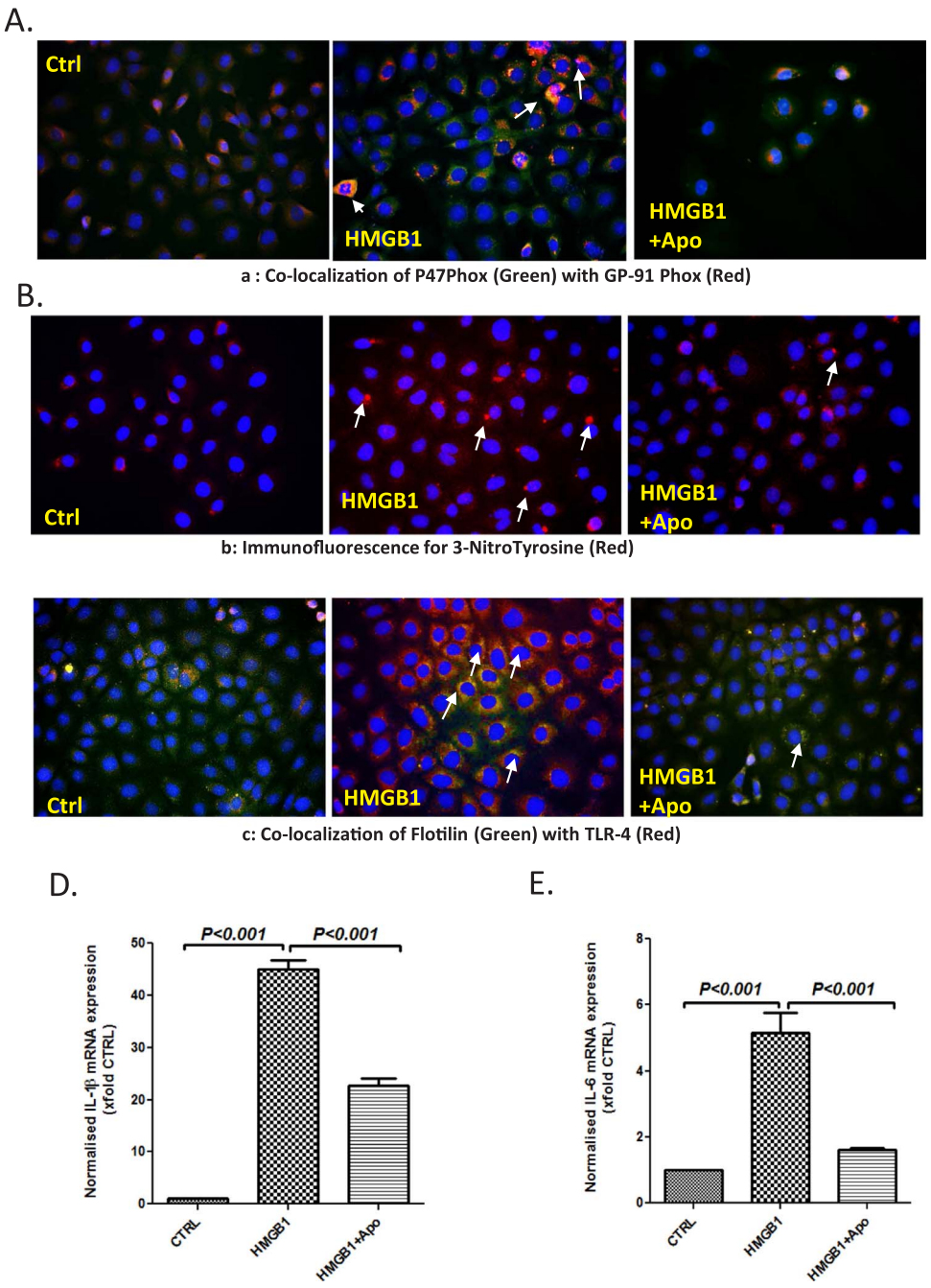


**Fig. 3.** HMGB1 leads to TLR-4 recruitment and activation via NADPH oxidase in IEC-6 cells. A. Immunofluorescence for P47Phox (Green) and GP-91 Phox (Red) co-localization in intestinal epithelial cells (IEC-6) treated with HMGB1 30 ng/ml (HMGB1), and HMGB1 + Apocynin 100 μM (HMGB1 + Apo) (40× images). B. Immunofluorescence for 3-Nitro-Tyrosine (Red) in intestinal epithelial cells (IEC-6) treated with HMGB1 30 ng/ml (HMGB1), and HMGB1 + Apocynin 100 μM (HMGB1 + Apo) (40× images). C. Immunofluorescence for Flotilin (Green) and TLR-4 (Red) co-localization in intestinal epithelial cells (IEC-6) treated with HMGB1 30 ng/ml (HMGB1), and HMGB1 + Apocynin 100 μM (HMGB1 + Apo) (40× images). D and E. mRNA expressions of IL-1β and IL-6 in intestinal epithelial cells (IEC-6) treated with HMGB1 30 ng/ml (HMGB1), and HMGB1 + Apocynin 100 μM (HMGB1 + Apo) as assessed by quantitative real time PCR, the expressions were normalized with 18 s and compared to the control group and represented as fold changes to Ctrl (**P < 0.05, ***P < 0.01). (For interpretation of the references to color in this figure legend, the reader is referred to the web version of this article.)

intestinal cells. Results showed that HMGB1 primed cells showed significant increase in TLR4-Flotillin colocalization that was blunted in the presence of a specific RAGE antagonist and use of denatured HMGB1 (Fig. 6A and Supplementary material Fig. 6A). Use of RAGE antagonist blunted TLR4 flotillin colocalization also implied that HMGB1-binding to TLR4 was not a predominant pathway in the IE6 cells (Fig. 6A). The significant ($p < 0.001$) increase in IL1β and IL6 mRNA expression by IE6 cells following HMGB1 priming was significantly decreased ($p < 0.001$) using specific antagonist against RAGE and the use of denatured HMGB1 suggesting that HMGB1-RAGE binding was instrumental in proinflammatory cytokine expression (Fig. 6B and C). Since monocyte chemoattractant protein (MCP1) also plays a role in an inflammatory microenvironment, mRNA expression analysis of MCP1 was assayed in IE6 cells. Results showed that MCP1 expression was significantly increased ($p < 0.001$) following HMGB1 priming (> 40 fold) when compared to vehicle controls (Fig. 6D). Use of an antagonist for RAGE or use of denatured HMGB1 which has lost its binding ability to RAGE significantly ($p < 0.001$) decreased expression of MCP1 mRNA suggesting that HMGB1-RAGE interaction increased possibility of a proinflammatory microenvironment (Fig. 6D).

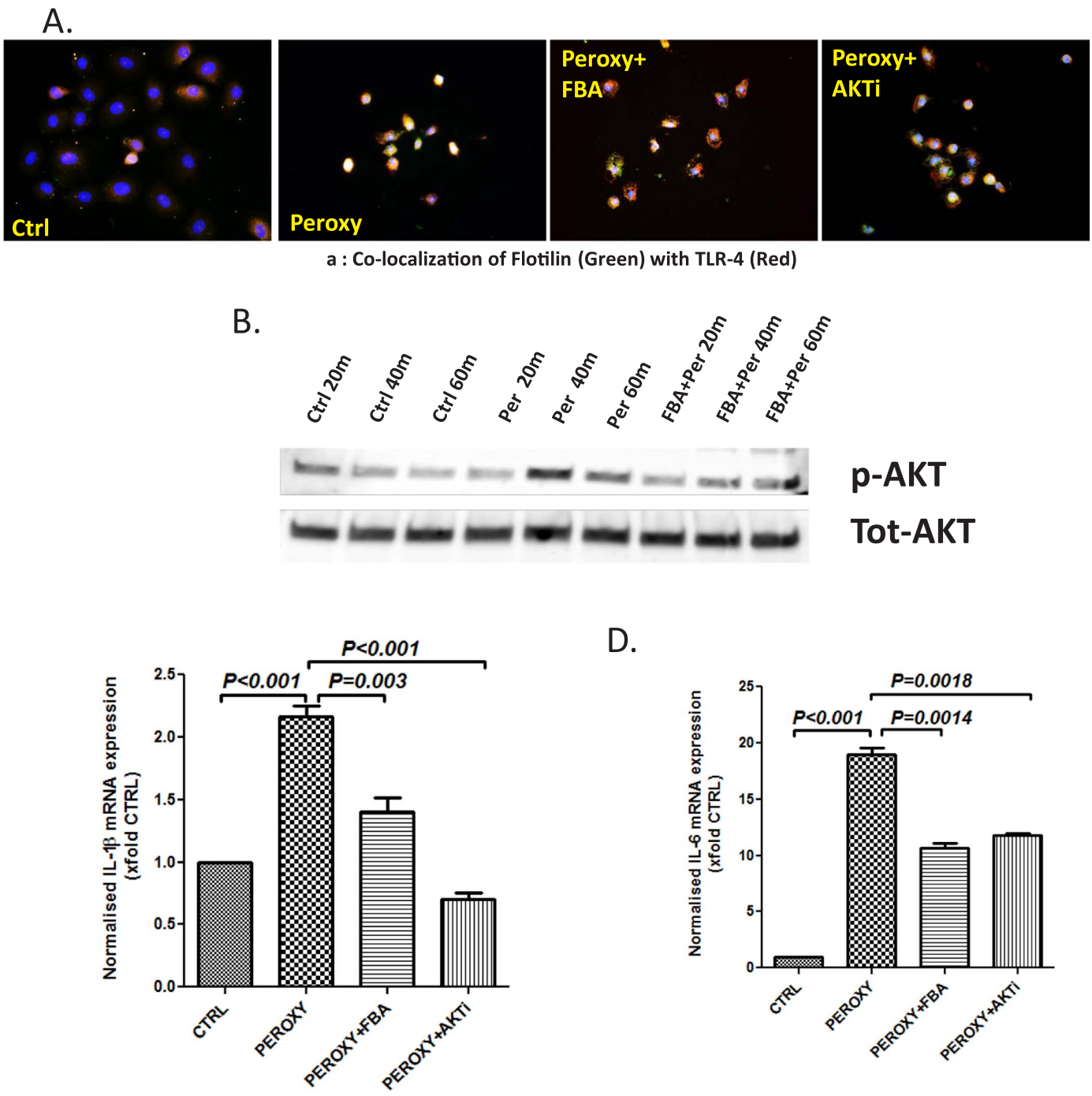


**Fig. 4.** Peroxynitrite leads to TLR-4 recruitment and activation by phosphorylation of AKT. A. Immunofluorescence for Flotilin (Green) and TLR-4 (Red) co-localization in intestinal epithelial cells (IEC-6) treated with peroxynitrite 300 μM (Peroxy) and combinations with phenyl Boronic acid 100 μM (Peroxy + FBA) and AKT inhibitor 10 μM (Peroxy + AKTi) (40× images). B. Western blot analysis of p-AKT protein levels in IEC-6 cells treated with peroxynitrite with and without Phenylboronic acid. Lanes 1–3 represent Control samples, Lanes 4–6 represent cells treated with peroxynitrite 300 μM and Lanes 7–9 represent cells treated with peroxynitrite and phenylboronic acid 100 μM. Proteins were harvested at 20 m, 40 m and 60 m time interval. The bands obtained were normalized to Total AKT. C and D. mRNA expressions of IL-1β and IL-6 in intestinal epithelial cells (IEC-6) treated with peroxynitrite 300 μM, and combinations with Phenyl Boronic acid 100 μM and AKT inhibitor 10 μM. HMGB1 + Apocynin 100 μM as assessed by quantitative real time PCR, the expressions were normalized with 18 s and compared to the control group and represented as fold changes to Ctrl (**P < 0.05, ***P < 0.01). (For interpretation of the references to color in this figure legend, the reader is referred to the web version of this article.)

## 4. Discussion

We present a novel pathological pathway of ectopic inflammation in the intestine following development of progressive NAFLD that is mediated by a) circulatory HMGB1-RAGE interaction and b) NOX2-Peroxynitrite-mediated TLR4 activation. The HMGB1-RAGE-mediated NOX2 activation and subsequent peroxynitrite induced TLR4 trafficking into the lipid rafts caused higher expression of IL1β and IL6 followed by increased release of MCP-1, a chemokine known to attract neutrophils.

NAFLD and its progressive inflammatory phase nonalcoholic steatohepatitis has been associated with intestinal inflammation resembling an IBD phenotype and colonic neoplasia [2]. Interestingly, steatosis or benign fat deposition in the liver was not found to be associated with neoplasia [2]. Our results where DIO group represented a benign steatosis group showed no intestinal inflammation or cytokine release thus conforming to the clinical data. This event may be ascribed to less

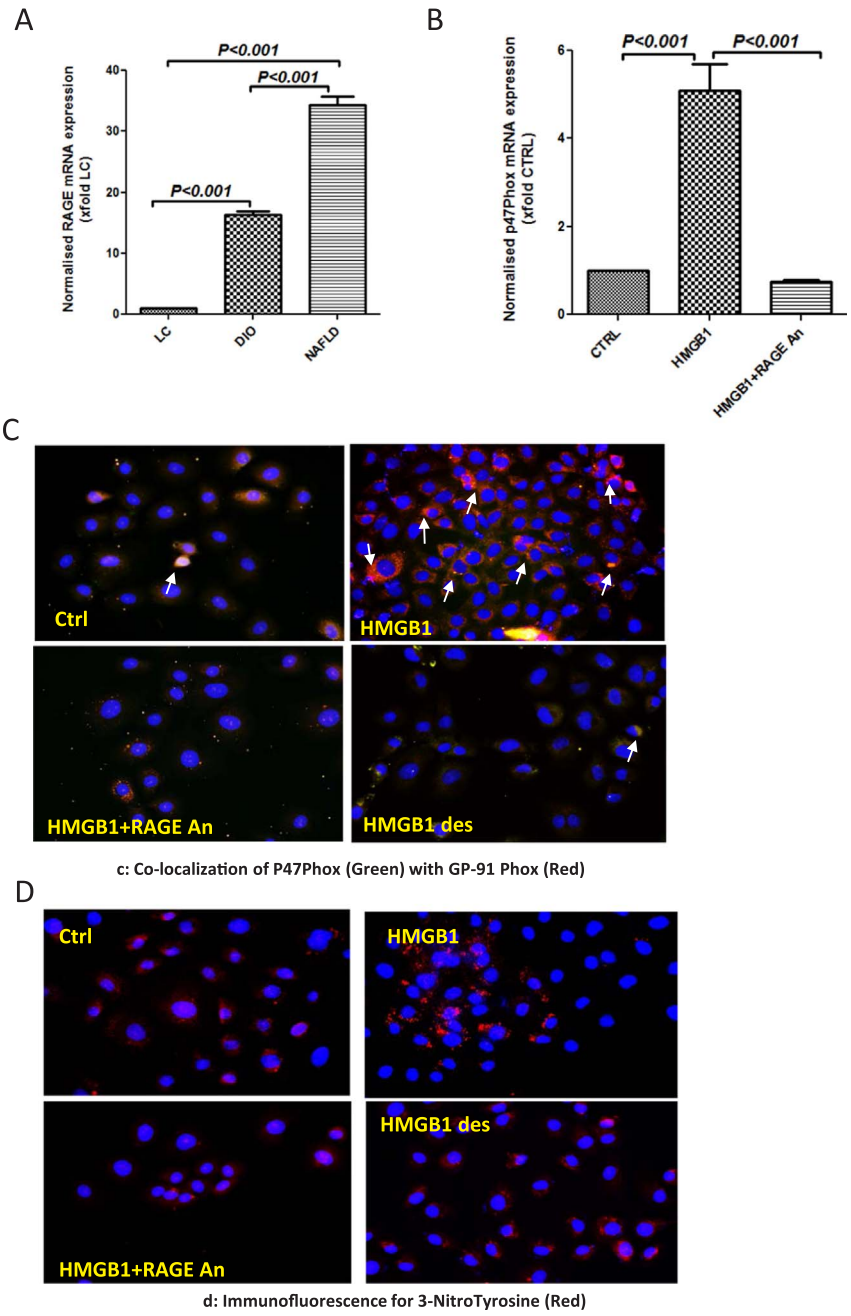


**Fig. 5.** HMGB1 generates peroxynitrite via NADPH oxidase by specifically binding to RAGE. A. mRNA expressions of RAGE in intestinal tissue of LC, DIO and NAFLD groups of mice as assessed by quantitative real time PCR, the expressions were normalized with 18 s and compared to the LC group and represented as fold changes to LC (**P < 0.05, ***P < 0.01). B. mRNA expressions of P47Phox in intestinal epithelial cells (IEC-6) treated with HMGB1 30 ng/ml (HMGB1), and HMGB1 + RAGE Antagonist 200 nM (HMGB1 + RAGEAn) as assessed by quantitative real time PCR, the expressions were normalized with 18 s and compared to the control group and represented as fold changes to Ctrl (**P < 0.05, ***P < 0.01). C. Immunofluorescence for P47Phox (Green) and GP-91 Phox (Red) co-localization in intestinal epithelial cells (IEC-6) treated with HMGB1 30 ng/ml (HMGB1), HMGB1 + RAGE Antagonist 200 nM (HMGB1 + RAGE An) and denatured HMGB1 30 ng/ml (HMGB1 des) (40× images). D. Immunofluorescence for 3-Nitro-tyrosine (Red) co-localization in intestinal epithelial cells (IEC-6) treated with HMGB1 30 ng/ml (HMGB1), HMGB1 + RAGE Antagonist 200 nM (HMGB1 + RAGE An) and denatured HMGB1 30 ng/ml (HMGB1 des) (40× images). (For interpretation of the references to color in this figure legend, the reader is referred to the web version of this article.)

HMGB1 in the liver and subsequent decreased circulatory HMGB1 levels following decreased liver cell necrosis. Thus, a progressive NAFLD with lobular inflammation as seen in our results paves way for higher circulatory HMGB1 and is a ligand for a series of proinflammatory events in the intestinal epithelial cells. The results also link the strong inflammatory phenotype observed in NAFLD intestines in our studies.

Though a strong association was observed in patients with NAFLD/NASH to development of colonic inflammation or studies that found NAFLD associations with IBD phenotype, the mechanisms that link these two inflammatory events were unclear [2,3]. Interestingly, there are considerable reports of circulatory cytokines, lack of adiponectin or increased leptin in NAFLD that are proinflammatory in nature but a direct mechanistic link to colonic inflammation is scarce [28]. Our observation that high circulatory HMGB1 in absence of significant other organ injuries probably originates in the damaged liver bodes well for a prominent role of this DAMP in causing ectopic intestinal inflammation. DAMPS has been found to play a prominent role in inflammation in many diseases [29]. However caution should be exercised when interpreting the data since prolonged feeding with high fat diet has

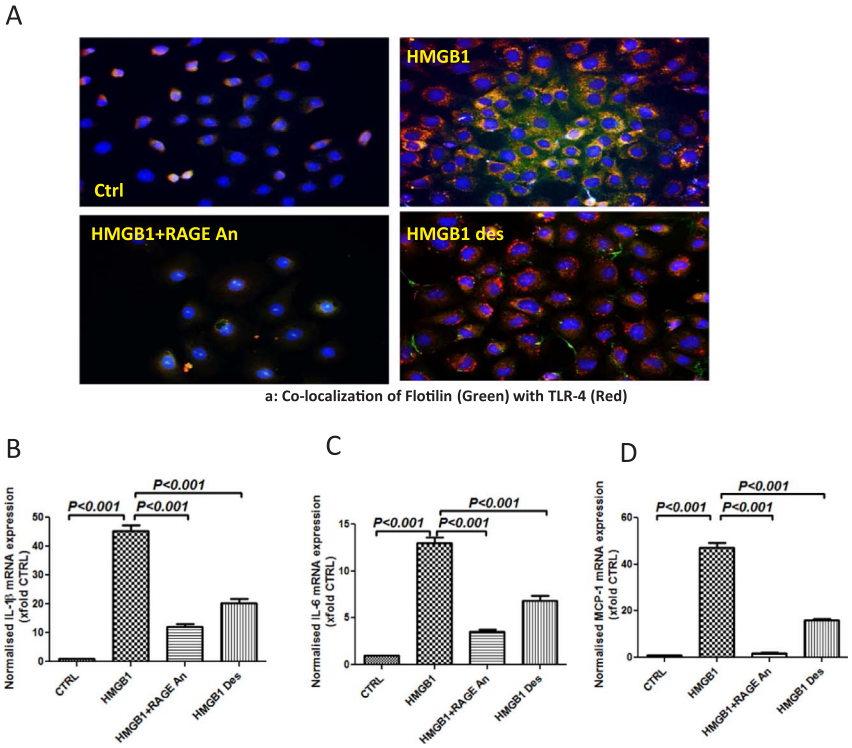


**Fig. 6.** HMGB1 recruits and activates TLR-4 by binding to RAGE. A. Immunofluorescence for Flotilin (Green) and TLR-4 (Red) co-localization in intestinal epithelial cells (IEC-6) treated with HMGB1 30 ng/ml (HMGB1), HMGB1 + RAGE Antagonist 200 nM (HMGB1 + RAGE An) and denatured HMGB1 30 ng/ml (HMGB1 des) (40× images). B–D. mRNA expressions of IL-1β, IL-6 and MCP-1 in intestinal epithelial cells (IEC-6) treated with HMGB1 30 ng/ml (HMGB1), and HMGB1 + Apocynin 100 μM (HMGB1 + Apo) as assessed by quantitative real time PCR, the expressions were normalized with 18 s and compared to the control group and represented as fold changes to Ctrl (**P < 0.05, ***P < 0.01). (For interpretation of the references to color in this figure legend, the reader is referred to the web version of this article.)

been associated with inflammatory lesions in the intestine [30]. Further the present study is limited in specifying the role of circulatory HMGB1 in causing ectopic inflammation in the intestine since we have unpublished data where intestinal HMGB1 was markedly increased following high fat feeding though it was significantly less than the circulatory levels of HMGB1. Future studies would have to focus on generating models that would clearly illustrate the source of HMGB1. Sterile inflammation in the liver is found to be associated with HMGB1 and other DAMPs [31]. The above fact is supported by our results that show liver HMGB1 levels are significantly high in NAFLD and little or no HMGB1 protein levels were detectable in the heart or kidney in our model of high fat fed mouse model of NAFLD.

HMGB1 is known for its proinflamamtory role in the intestine and other tissues including liver [10,31,32]. High circulatory levels of HMGB1 was associated with increased expression of proinflammatory mediators IL1β, MCP1, TGF-β and IFN-γ [11,33]. High HMGB1 was also associated with NOX2 activation and increased 3-nitro tyrosine formation, a marker of peroxynitrite-mediated nitrative stress [34–36]. The above events decreased significantly in p47 phox knockout mice. Peroxynitrite formation and TLR4 trafficking to the lipid rafts also decreased in P47 phox knockout mice thus indicating that the proinflammatory events including TLR4 trafficking was dependent on NOX2. This was intriguing since HMGB1 is known to bind TLR4 in generating a proinflammatory cascade. Our results also implied that if HMGB1 and redox signaling events were to generate an inflammatory phenotype in the intestine, it had to do so by activating NOX2. Studies suggest that HMGB1 can induce an activation of NOX2 by a Mac-1 dependent pathway but in contrast can also induce phosphorylation of p40 subunit of NOX2, thereby inhibiting its activation through a RAGE dependent pathway in neutrophils [36,37]. With HMGB1 levels being associated with increased NOX2 activation in the intestine we resorted to study the redox pathway of inducing TLR4 signaling in our studies. Results showed that HMGB1-primed intestinal epithelial cells activated NOX2, formed higher nitration of tyrosine residues, increased TLR4 trafficking into lipid rafts and caused higher expression of proinflammatory cytokines IL1β and IL6, events that were blocked by use of NOX2 inhibitor apocynin. Thus, HMGB1-NOX2 activation was upstream to TLR4 activation and the results opened the possibility of a non-TLR4 based mechanism in our studies. Use of AKT inhibitor also blocked peroxynitrite mediated TLR4 trafficking suggesting NOX2-peroxynitrite-AKT signaling as a primary pathway for TLR4-mediated inflammation in the intestinal epithelial cells.

RAGE has been found to bind HMGB1 in the B box binding region [19]. The three redox states of HMGB1 differ by structure, half-life, and activity. The redox states determine the stability of HMGB1 and its binding to either RAGE or TLR4 [19]. We found higher RAGE expression in the NAFLD intestines. Our results also showed decreased NOX2 activation, peroxynitrite formation, TLR4 trafficking and proinflammatory mediator expression in RAGE antagonist treated HMGB1 primed intestinal epithelial cells suggesting strongly that HMGB1 mediates its effect through RAGE binding. Further the decreased and almost negligible TLR4 trafficking in the presence of RAGE antagonist proved that HMGB1-RAGE binding but not HMGB1-TLR4 caused the inflammatory events in the cells. HMGB1 mediated effects were further confirmed using denatured HMGB1 primed cells.

Though our results support strongly the involvement of circulatory HMGB1-mediated inflammation in the NAFLD intestine, several questions remain unanswered. Firstly a high fat diet induced NAFLD model that we have used in the present study is a slow and progressive inducer of liver disease pathology [38]. Such models cause obesity and insulin resistance and has been shown to alter gut microbiome and dysbiosis. It is shown in clinical studies that dysbiosis is associated with IBD like phenotype which can cause liver disease by itself [3,28]. This fact complicates our interpretation that HMGB1 was primarily derived from liver and did not originate from the intestine. Most murine models of NAFLD cause gut dysbiosis and there is hardly a way that a liver disease

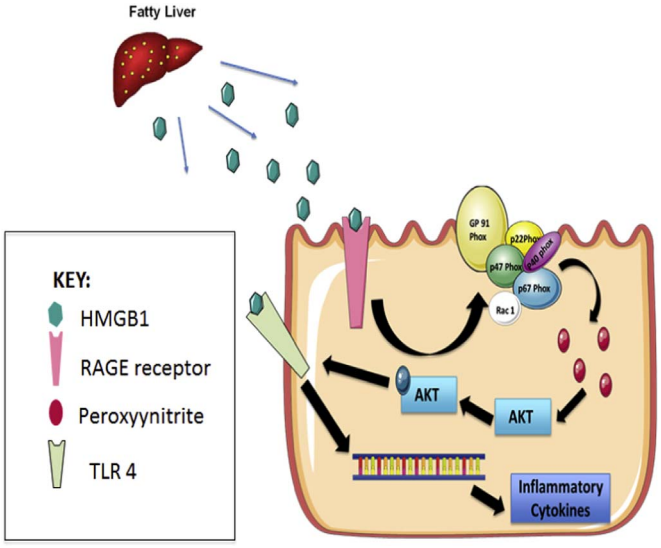


**Fig. 7.** HMGB1 released from NAFLD liver reaches and binds to RAGE receptors in the intestines activating it via circulation, leading to NADPH oxidase complex assembly on the membrane generating Peroxynitrite, The Peroxynitrite thus generated phosphorylates AKT leading to TLR-4 recruitment in the lipid rafts in the cell membrane, where it can bind to HMGB1 leading to transcription of inflammatory cytokines such as IL-6 and IL-1β.

phenotype is established where the intestine is unaffected. Secondly, HMGB1-TLR4 pathway is favored because of the increased stability of HMGB1 [19]. This event does not rule out the HMGB1-TLR4-mediated inflammation in other cell types of the intestine since we studied the pathways only in the intestinal epithelial cells.

Taken together, our data in both an in vivo and in vitro setting shows a novel HMGB1-RAGE mediated redox signaling pathway that exerts its effect through peroxynitrite induced AKT phosphorylation which in turn directs TLR4 to lipid rafts (Fig. 7). The ensuing event caused uninterrupted inflammation through release of IL1β, IL6 and MCP1 and resulted in an IBD-like phenotype. With recent published studies including ours showing the efficacy of specific peroxynitrite scavenger phenyl boronic acid (FBA) in curbing NAFLD mediated inflammation, it will be justified to assume that FBA may be a likely candidate for an interventional strategy to curb ectopic inflammatory events in NAFLD or IBD itself [26]. The present study also finds a probable mechanistic link to NAFLD induced intestinal neoplasia since chronic inflammation such as that in NAFLD is deemed to be paramount to such an event in humans.

## Grant support

This work has been supported by NIH Pathway to Independence Award, R00ES019875, P30GM103336 and P01AT003961 to Saurabh Chatterjee, R01DK053792 to Anna Mae Diehl.

## Conflict of interest

The authors declare that there is no conflict of interest.

## Acknowledgement

The authors gratefully acknowledge the technical services of Benny Davidson at the IRF, University of South Carolina School of Medicine and AML Labs (Baltimore MD). Our special thanks to Dr. Suvarthi Das for help with interpretation and technical guidance for cytochemistry. We also thank the Instrumentation resource facility (IRF) at the University of South Carolina for equipment usage and consulting services.

## Appendix A. Supplementary material

Supplementary data associated with this article can be found in the online version at http://dx.doi.org/10.1016/j.redox.2017.05.005.

## References

[1] M.N. VanSaun, I.K. Lee, M.K. Washington, L. Matrisian, D.L. Gorden, High fat diet induced hepatic steatosis establishes a permissive microenvironment for colorectal metastases and promotes primary dysplasia in a murine model, Am. J. Pathol. 175 (2009) 355–364.
[2] V.W. Wong, G.L. Wong, S.W. Tsang, T. Fan, W.C. Chu, J. Woo, et al., High prevalence of colorectal neoplasm in patients with non-alcoholic steatohepatitis, Gut 60 (2011) 829–836.
[3] C.Y. Chao, R. Battat, A. Al Khoury, S. Restellini, G. Sebastiani, T. Bessissow, Co-existence of non-alcoholic fatty liver disease and inflammatory bowel disease: a review article, World J. Gastroenterol.: WJG 22 (2016) 7727–7734.
[4] L.A. Adams, Q.M. Anstee, H. Tilg, G. Targher, Non-alcoholic fatty liver disease and its relationship with cardiovascular disease and other extrahepatic diseases, Gut (2017).
[5] H. Tilg, A.M. Diehl, NAFLD and extrahepatic cancers: have a look at the colon, Gut 60 (2011) 745–746.
[6] S. Chatterjee, D. Ganini, E.J. Tokar, A. Kumar, S. Das, J. Corbett, et al., Leptin is key to peroxynitrite-mediated oxidative stress and Kupffer cell activation in experimental nonalcoholic steatohepatitis, J. Hepatol. (2012).
[7] K. Guo, J.E. McMinn, T. Ludwig, Y.H. Yu, G. Yang, L. Chen, et al., Disruption of peripheral leptin signaling in mice results in hyperleptinemia without associated metabolic abnormalities, Endocrinology 148 (2007) 3987–3997.
[8] X. Guo, M.R. Roberts, S.M. Becker, B. Podd, Y. Zhang, S.C. Chua Jret al., Leptin signaling in intestinal epithelium mediates resistance to enteric infection by Entamoeba histolytica, Mucosal Immunol. 4 (2011) 294–303.
[9] F. Alhasson, D. Dattaroy, S. Das, V. Chandrashekaran, R.K. Seth, R.G. Schnellmann, et al., NKT cell modulates NAFLD potentiation of metabolic oxidative stress-induced mesangial cell activation and proximal tubular toxicity, Am. J. Physiol. Ren. Physiol. 310 (2016) F85–F101.
[10] A. Alisi, R. Carsetti, V. Nobili, Pathogen- or damage-associated molecular patterns during nonalcoholic fatty liver disease development, Hepatology 54 (2011) 1500–1502.
[11] M. Ganz, T.N. Bukong, T. Csak, B. Saha, J.K. Park, A. Ambade, et al., Progression of non-alcoholic steatosis to steatohepatitis and fibrosis parallels cumulative accumulation of danger signals that promote inflammation and liver tumors in a high fat-cholesterol-sugar diet model in mice, J. Transl. Med. 13 (2015) 193.
[12] L. Li, L. Chen, L. Hu, Nuclear factor high-mobility group box 1 mediating the activation of Toll-like receptor 4 signaling in hepatocytes in the early stage of non-alcoholic fatty liver disease in mice, J. Clin. Exp. Hepatol. 1 (2011) 123–124.
[13] L. Li, L. Chen, L. Hu, Y. Liu, H.Y. Sun, J. Tang, et al., Nuclear factor high-mobility group box 1 mediating the activation of Toll-like receptor 4 signaling in hepatocytes in the early stage of nonalcoholic fatty liver disease in mice, Hepatology 54 (2011) 1620–1630.
[14] Y.S. Roh, E. Seki, Toll-like receptors in alcoholic liver disease, non-alcoholic steatohepatitis and carcinogenesis, J. Gastroenterol. Hepatol. 28 (Suppl 1) (2013) S38–S42.
[15] R.K. Seth, S. Das, D. Dattaroy, V. Chandrashekaran, F. Alhasson, G. Michelotti, et al., TRPV4 activation of endothelial nitric oxide synthase resists nonalcoholic fatty liver disease by blocking CYP2E1-mediated redox toxicity, Free Radic. Biol. Med. 102 (2016) 260–273.
[16] W. Zeng, W. Shan, L. Gao, D. Gao, Y. Hu, G. Wang, et al., Inhibition of HMGB1 release via salvianolic acid B-mediated SIRT1 up-regulation protects rats against non-alcoholic fatty liver disease, Sci. Rep. 5 (2015) 16013.
[17] W. Zhang, L.W. Wang, L.K. Wang, X. Li, H. Zhang, L.P. Luo, et al., Betaine protects against high-fat-diet-induced liver injury by inhibition of high-mobility group box 1 and Toll-like receptor 4 expression in rats, Dig. Dis. Sci. 58 (2013) 3198–3206.
[18] L.T. Gan, D.M. Van Rooyen, M.E. Koina, R.S. McCuskey, N.C. Teoh, G.C. Farrell, Hepatocyte free cholesterol lipotoxicity results from JNK1-mediated mitochondrial injury and is HMGB1 and TLR4-dependent, J. Hepatol. 61 (2014) 1376–1384.
[19] D.J. Weber, Y.M. Allette, D.S. Wilkes, F.A. White, The HMGB1-RAGE inflammatory pathway: implications for brain injury-induced pulmonary dysfunction, Antioxid. Redox Signal. 23 (2015) 1316–1328.
[20] H.S. Tong, Y.Q. Tang, Y. Chen, J.M. Qiu, Q. Wen, L. Su, Early elevated HMGB1 level predicting the outcome in exertional heatstroke, J. Trauma 71 (2011) 808–814.
[21] M. Fujioka, T. Nakano, K. Hayakawa, K. Irie, Y. Akitake, Y. Sakamoto, et al., ADAMTS13 gene deletion enhances plasma high-mobility group box 1 elevation and neuroinflammation in brain ischemia-reperfusion injury, Neurol. Sci.: Off. J. Ital. Neurol. Soc. Ital. Soc. Clin. Neurophysiol. 33 (2012) 1107–1115.
[22] C. Ingels, I. Derese, P.J. Wouters, G. Van den Berghe, I. Vanhorebeek, Soluble RAGE and the RAGE ligands HMGB1 and S100A12 in critical illness: impact of glycemic control with insulin and relation with clinical outcome, Shock (Augusta, Ga) 43 (2015) 109–116.
[23] T. Ito, K. Kawahara, K. Okamoto, S. Yamada, M. Yasuda, H. Imaizumi, et al., Proteolytic cleavage of high mobility group box 1 protein by thrombin-thrombomodulin complexes, Arterioscler. Thromb. Vasc. Biol. 28 (2008) 1825–1830.
[24] Y. Sakamoto, K. Mashiko, H. Matsumoto, Y. Hara, N. Kutsukata, Y. Yamamoto, Relationship between effect of polymyxin B-immobilized fiber and high-mobility group box-1 protein in septic shock patients, ASAIO J. (Am. Soc. Artif. Intern.

Organs: 1992) 53 (2007) 324–328.
[25] K. Tagami, T. Yujiri, A. Tanimura, N. Mitani, Y. Nakamura, K. Ariyoshi, et al., Elevation of serum high-mobility group box 1 protein during granulocyte colony-stimulating factor-induced peripheral blood stem cell mobilisation, Br. J. Haematol. 135 (2006) 567–569.
[26] S. Das, F. Alhasson, D. Dattaroy, S. Pourhoseini, R.K. Seth, M. Nagarkatti, et al., NADPH oxidase-derived peroxynitrite drives inflammation in mice and human nonalcoholic steatohepatitis via TLR4-lipid raft recruitment, Am. J. Pathol. (2015).
[27] D.P. McKernan, G. Gaszner, E.M. Quigley, J.F. Cryan, T.G. Dinan, Altered peripheral toll-like receptor responses in the irritable bowel syndrome, Aliment. Pharmacol. Ther. 33 (2011) 1045–1052.
[28] A. Scalera, M.N. Di Minno, G. Tarantino, What does irritable bowel syndrome share with non-alcoholic fatty liver disease? World J. Gastroenterol.: WJG 19 (2013) 5402–5420.
[29] I. Garcia-Martinez, M.E. Shaker, W.Z. Mehal, Therapeutic opportunities in damage-associated molecular pattern-driven metabolic diseases, Antioxid. Redox Signal. 23 (2015) 1305–1315.
[30] D. Owczarek, T. Rodacki, R. Domagala-Rodacka, D. Cibor, T. Mach, Diet and nutritional factors in inflammatory bowel diseases, World J. Gastroenterol.: WJG 22 (2016) 895–905.
[31] P. Kubes, W.Z. Mehal, Sterile inflammation in the liver, Gastroenterology 143 (2012) 1158–1172.
[32] Z. Hu, X. Wang, L. Gong, G. Wu, X. Peng, X. Tang, Role of high-mobility group box 1 protein in inflammatory bowel disease, Inflamm. Res.: Off. J. Eur. Histamine Res. Soc. [et al.] 64 (2015) 557–563.
[33] G.P. Sims, D.C. Rowe, S.T. Rietdijk, R. Herbst, A.J. Coyle, HMGB1 and RAGE in inflammation and cancer, Annu. Rev. Immunol. 28 (2010) 367–388.
[34] J. Fan, Y. Li, R.M. Levy, J.J. Fan, D.J. Hackam, Y. Vodovotz, et al., Hemorrhagic shock induces NAD(P)H oxidase activation in neutrophils: role of HMGB1-TLR4 signaling, J. Immunol. 178 (2007) 6573–6580.
[35] C. Janko, M. Filipovic, L.E. Munoz, C. Schorn, G. Schett, I. Ivanovic-Burmazovic, et al., Redox modulation of HMGB1-related signaling, Antioxid. Redox Signal. 20 (2014) 1075–1085.
[36] J.M. Tadie, H.B. Bae, S. Banerjee, J.W. Zmijewski, E. Abraham, Differential activation of RAGE by HMGB1 modulates neutrophil-associated NADPH oxidase activity and bacterial killing, Am. J. Physiol. Cell Physiol. 302 (2012) C249–C256.
[37] H.M. Gao, H. Zhou, F. Zhang, B.C. Wilson, W. Kam, J.S. Hong, HMGB1 acts on microglia Mac1 to mediate chronic neuroinflammation that drives progressive neurodegeneration, J. Neurosci.: Off. J. Soc. Neurosci. 31 (2011) 1081–1092.
[38] M.A. Abdelmegeed, A. Banerjee, S.H. Yoo, S. Jang, F.J. Gonzalez, B.J. Song, Critical role of cytochrome P450 2E1 (CYP2E1) in the development of high fat-induced non-alcoholic steatohepatitis, J. Hepatol. 57 (2012) 860–866.